

M. Derrick

Argonne National Laboratory, Argonne, IL 60439

Introduction

Charged particle multiplicities in hadronic collision have been measured for all energies up to $\sqrt{s} = 540$ GeV in the center of mass. Similar measurements in e^+e^- annihilation cover the much smaller range - up to $\sqrt{s} = 40$ GeV. Data is also available from deep inelastic neutrino scattering up to $\sqrt{s} \sim 10$ GeV.

The experiments measure the mean charged multiplicity $\langle N_{ch} \rangle$, the rapidity density at $y = 0$, and the distributions in prong number. The mean number of photons associated with the events can be used to measure the η^0 and π^0 multiplicities. Some information is also available on the charged pion, kaon, and nucleon fractions as well as the K^0 and Λ^0 rates and for the higher energy data, the Ξ fraction. We review this data and consider the implications of extrapolations to SSC energies.

Multiplicities

A fit to the available data on $\langle N_{ch} \rangle$ for pp collisions using the form

$$\langle N_{ch} \rangle = a + b \ln s + c \ln^2 s \quad (1)$$

which represents the data up to ISR energies well gives $a = 0.88 \pm 0.10$, $b = 0.44 \pm 0.05$, and $c = 0.118 \pm 0.006$ for \sqrt{s} in GeV. This parameterization, shown by the full line in Fig. 1, gives $\langle N_{ch} \rangle = 25.1$ at $\sqrt{s} = 540$ GeV in good agreement with the value of 26.8 ± 2.1 reported by the UA5 collaboration. (2) An $a + b \ln s$ form would be appropriate if the rapidity density remained constant and rapidity plateau merely widened as the available energy increases. Since a $\ln^2 s$ term is required, this simple expectation is not valid. At 40 TeV in the center of mass, Eq. (1) gives $\langle N_{ch} \rangle = 63.2$. This extrapolation may be an underestimate since the fraction of hard collisions which tend to populate the central region is increasing rapidly with energy and approaches unity for SSC energies.

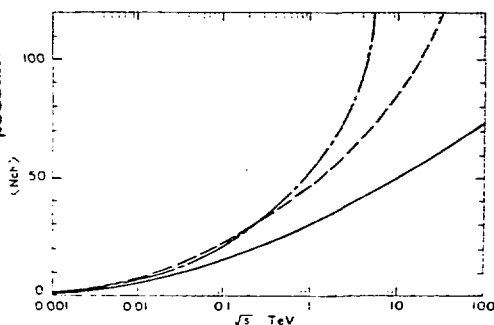


Fig. 1. Mean charged multiplicity in pp collisions (full line) and e^+e^- annihilation according to two parameterizations (dashed line and dashed-dotted line).

The e^+e^- data shows a somewhat faster increase with energy. A fit of the PETRA data (3) to Eq. (1)

gives $a = 3.33 \pm 0.11$, $b = -0.4 \pm 0.08$, and $c = 0.26 \pm 0.01$, shown as a dashed line in Fig. 1. The expected asymptotic behavior of $\langle N_{ch} \rangle$ in QCD (4) is

$$\langle N_{ch} \rangle = a \left(\ln \frac{Q}{\Lambda} \right)^b \exp \left(c \ln \frac{Q}{\Lambda} \right)^{1/2} \quad (2)$$

where for five flavors $b = -0.492$ and $c = 6.26$ with $\Lambda = 0.25$ GeV. (5) Normalizing at $\sqrt{s} = 29$ GeV to the HRS measurement (5) of $\langle N_{ch} \rangle = 11.7$ after removing charged particles from K^0 and Λ decay, gives $a = 0.108$. The parameterization is shown as the dashed-dotted line in Fig. 1. Both e^+e^- parameterizations give similar predictions up to 1 TeV, which is the region of interest for high P_T jets at the SSC.

If events with two very high P_T jets gave multiplicities that just resulted from the addition of two e^+e^- jets to a minimum bias hadronic event, then the charged multiplicities for an event with, say, two 0.5 TeV jets would be $\sim 80 + 63 = 143$ charged particles. This is almost certainly an underestimate as it ignores all initial state radiation effects as well as the possibility of the spectator partons also being forced off shell and so radiating.

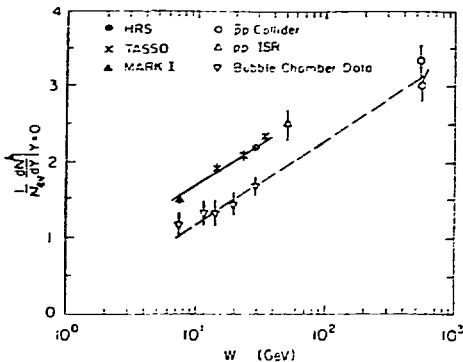


Fig. 2. Energy variation of rapidity density at $y=0$ for e^+e^- annihilation (full line) and pp collisions (dashed line).

The rapidity density at $y = 0$ increases with \sqrt{s} as $a + b \ln \sqrt{s}$, as shown in Fig. 2. (5) Extrapolating this data to $\sqrt{s} = 40$ TeV gives $dn/dy = 5.5$ charged particles per unit of rapidity near $y = 0$.

At high energies, the number of γ rays increases linearly with N_{ch} . At $\sqrt{s} = 0.54$ TeV, the data (6) can be fit by :

$$N_\gamma = (8 \pm 3) + (0.90 \pm 0.08) N_{ch} \quad (3)$$

The correlation is similar to, but stronger than, that observed at Fermilab and ISR energies.

Heavy Particle Fractions

The fraction of heavier particles grows up with energy as shown in Fig. 3 with ratios $K/\pi \sim 12\%$ and $\bar{p}/\pi \sim 6\%$ at 0.54 TeV. The lower energy e^+e^- data have relatively more heavy particles: for example, at 30

[Handwritten signature]

PORTIONS OF THIS REPORT ARE ILLEGIBLE. It has been reproduced from the best available copy to permit the broadest possible availability.

GeV the average event contains $10 \pi^{\pm}$, $1.8 K^{\pm}$, $1.8 K^0$, $0.7 p\bar{p}$ and 0.025Ξ . A recent observation of Ξ production by UAS group⁽⁶⁾ of 0.08 ± 0.03 , however, is significantly higher than the above e^+e^- value.

The $\langle p_T \rangle$ value grows strongly above Fermilab energies, particularly for the heavier particles as shown in Fig. 4.⁽⁹⁾

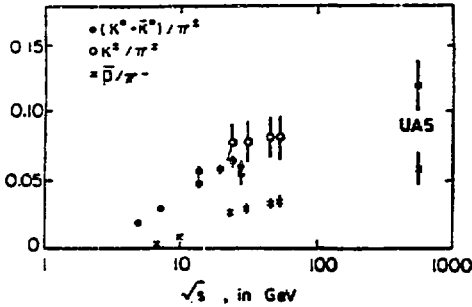


Fig. 3. Heavy particle fractions in pp and $\bar{p}p$ collisions.

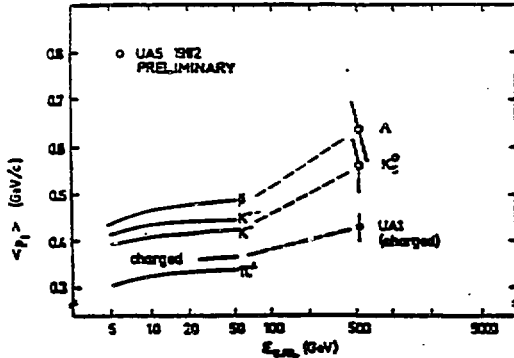


Fig. 4. $\langle p_T \rangle$ values in pp and $\bar{p}p$ collisions.

Multiplicity Distributions

The hard and soft collisions show a major difference in the shape of the multiplicity distributions. The hard collisions have a much narrower prong distribution than do the non-diffractive pp collisions. The $\langle N_{ch} \rangle / D$ ratio is ≈ 3 for e^+e^- annihilation and ≈ 2 for pp and $\bar{p}p$ collisions as shown in Fig. 5.⁽³⁾

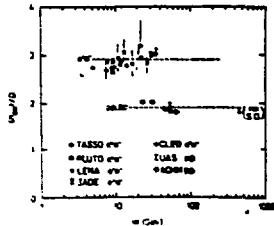


Fig. 5. $\langle N_{ch} \rangle / D$ ratios for e^+e^- annihilation and pp, $\bar{p}p$ collisions.

Each set of data, however, separately satisfies KNO scaling: if $Z = N_{ch} / \langle N_{ch} \rangle$, then $\langle N_{ch} \rangle / \langle \sigma_{ch} \rangle$ is a universal function $\psi(z)$.

Proton-proton data up to ISR energies satisfy this scaling quite well as shown by the energy variation of the moments $C_n = \langle n^q \rangle / \langle n \rangle^q$ in Fig. 6. At collider energies, however, the multiplicity distribution in the KNO form becomes much wider. Furthermore, as seen in Fig. 7, the central region $|\eta| < 0.5$ is even broader than the total distribution $|\eta| < 5.0$. Liu and Meng⁽⁸⁾ parameterize the KNO scale breaking in terms of a parameter α , where $\alpha = 1 - 6.8 / \langle N_{ch} \rangle^2$, so that at very high energies $\alpha \approx 1$ and $\psi(Z) \approx 4Ze^{-Z}$. This form fits the UAS data for $|\eta| < 0.5$. If this is indeed the asymptotic form, then events with $Z = 5$ or $\langle N_{ch} \rangle = 315$ will occur at the SSC with a frequency of 10^{-4} .

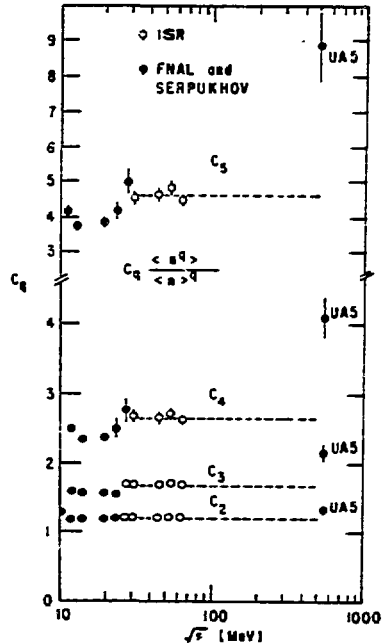


Fig. 6. Multiplicity distribution for pp/ $\bar{p}p$ collisions.

There have been various attempts at understanding the KNO scaling phenomena, none of them completely convincing. A broader distribution will obviously result from the addition of several distributions with different mean values. Diffractive and non-diffractive interactions provide examples of two such processes⁽⁹⁾ and, of course, the former is absent in e^+e^- annihilation. The dual model in which the number of chains increases with energy offers another good explanation.⁽¹⁰⁾

Carruthers and Shih⁽¹¹⁾ have pointed out that the UAS data can be fit with the negative binomial distribution, which in the KNO limit is:

$$\langle n \rangle = \frac{e^{-\alpha}}{(1-\alpha)^2} Z^{\alpha-1} e^{-\alpha Z} \quad (4)$$

This is the distribution expected from α , independent

identical sources with mean values $\langle n \rangle/\mu$. The UAS data is fit with $m = 3$, although $m = 2$, which gives the Liu and Meng form is also satisfactory. Present data does not measure a significant change of m with energy.

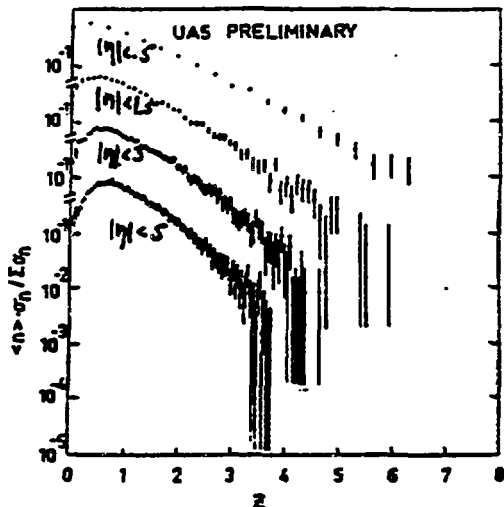


Fig. 7. KNO distribution for $\bar{p}p$ collisions at 540 GeV.

Correlations

A final major difference between e^+e^- data and hadronic beam jets is in the absence of forward-backward correlations in the former case as compared to the strong effects seen for the beam jets. The UAS data⁽¹²⁾ when fit by:

$$\langle N_F \rangle = a + b N_B \quad (5)$$

gives $b = 0.57 \pm 0.01$. The slope parameter decreases linearly as a larger and larger rapidity gap is imposed between the F and B regions, but $b \sim 0.1$ even for a rapidity gap of 6 units. A similar but weaker effect is seen in the ISR data.

The correlations on the rapidity plateau, however, in both e^+e^- data and for all of the hadronic data shows a similar short-range effect over ~ 1 unit of rapidity.

The hadronic F:B correlations, as well as the rapidity correlations can be jointly explained in a model of independent emission of low clusters.⁽¹³⁾ This model, however, does not obviously explain the difference with the e^+e^- results. At the SSC, many events will contain two jets coming from hard collisions as well as the beam jets and so will provide a laboratory for exploring these differences within a single experiment.

References

1. W. Thome et al., Nucl. Phys. 5129, 365 (1977).
2. K. Alpgard et al., Phys. Lett. 107B, 315, 319 (1981).
3. M. Altmoff et al., Z. Phys. 22, 307 (1984).

4. B. R. Webber, Nucl. Phys. 8238, 492 (1984).
5. D. Bender et al., "Study of Quark Fragmentation at 29 GeV: Global Jet Parameters and Single Particle Distributions," Phys. Rev. D.
6. J. Kuschbrooke, Proceedings of DPF workshop on DP Options for the Supercollider.
7. G. Arnison et al., Phys. Lett. 123B, 108 (1983). K. Alpgard et al., *ibid.*, 121d, 209 (1983).
8. L. S. Liu and T.-C. Meng, Phys. Rev. D27, 2640 (1983).
9. See, for example, S. J. Barish et al., Phys. Rev. D9, 2689 (1974).
10. A. Capella and J. Tran Than Van, Z. Phys. 23, 165 (1984).
11. P. Carruthers and C. C. Shih, Phys. Lett. 127B, 242 (1983). The authors (Phys. Lett. 137B, 425 (1984)) also point out that the difference between the narrow e^+e^- and the wide hadronic distributions can be understood if the latter have a smaller coherent component between the fundamental emitters.
12. Results presented at Lund Symposium on Multiparticle Dynamics.
13. K. Alpgard et al., Phys. Lett. 123B, 361 (1983).

DISCLAIMER

This report was prepared as an account of work sponsored by an agency of the United States Government. Neither the United States Government nor any agency thereof, nor any of their employees, makes any warranty, express or implied, or assumes any legal liability or responsibility for the accuracy, completeness, or usefulness of any information, apparatus, product, or process disclosed, or represents that its use would not infringe privately owned rights. Reference herein to any specific commercial product, process, or service by trade name, trademark, manufacturer, or otherwise does not necessarily constitute or imply its endorsement, recommendation, or favoring by the United States Government or any agency thereof. The views and opinions of authors expressed herein do not necessarily state or reflect those of the United States Government or any agency thereof.